

# Crystal Structure and Conformation of a Dipyrromethane. The *gem*-Dimethyl Effect

Derek A. Lightner, Adrienne K. Tipton, and David A. Lightner\*

Department of Chemistry, University of Nevada, Reno, Nevada 89557-0020, USA

**Summary.** A crystal structure determination of the new dipyrromethane diethyl-2,3,5,5,7,8-hexamethyl-5,10-dihydrodipyrroin-1,9-dicarboxylate (**1**) is only the third reported for a dipyrromethane and the first with a *gem*-dimethyl group at the bridging carbon atom. Conformation determining torsion angles are compared to those from molecular mechanics calculations and to the corresponding data for an analogous dipyrromethane (**2**) with no *gem*-dimethyl moiety. The crystal structures of **1** and **2** differ significantly: **1** adopts the *+ac,+ac* or *-ac,-ac* conformation, whereas **2** exists in the *-ac,+sc* conformation in an intermolecularly hydrogen bonded dimer. There is no evidence for hydrogen bonding in crystals of **1**, and its *ac* conformation is unlike that found about the central core of bilirubin (*sc,sc*). Taken collectively, the data indicate that the presence of a sterically demanding and potentially conformation distorting *gem*-dimethyl group located at the bridging carbon of a dipyrromethane (*i*) stabilizes a conformation that brings the pyrrole NH groups *syn* to the *gem*-dimethyls and (*ii*) would destabilize the ridge-tilt conformation of 10,10-dimethylbilirubin.

**Keywords.** Pyrroles; Stereochemistry; Molecular mechanics; Hydrogen bonding.

## Introduction

The dipyrromethane (5,10-dihydrodipyrroin) unit forms the central core of the important and structurally interesting mammalian natural product bilirubin (Fig. 1A) which is the yellow pigment of jaundice and the end product of heme metabolism in mammals [1–3]. Considerable effort has been devoted to understanding the properties and metabolism of bilirubin, with particular attention being focussed on carbon-carbon bond rotations within the dipyrromethane core that guide the pigment to fold into its most stable conformation which is shaped like a ridge-tile (Fig. 1B). The ridge-tile shape, with the dipyrromethane core in an *sc,sc* conformation, lies at an energy minimum for steric reasons [4,5] and is additionally stabilized by intramolecular hydrogen bonds linking carboxylic acids to opposing dipyrroinones [4–7]. In ordinary dipyrromethanes (Fig. 1C), conformational stabilization from hydrogen bonding is usually not possible, except when special circumstances ( $R^3 = \text{CO}_2\text{Et}$ ) permit intramolecular hydrogen bonds between the pyrrole-NH and ester-C=O as detected by IR spectroscopy. This type of hydrogen bonding is thought to stabilize a (gable) conformation where  $\phi_1 \sim \phi_2 \sim 90^\circ$  [8].

\* Corresponding author

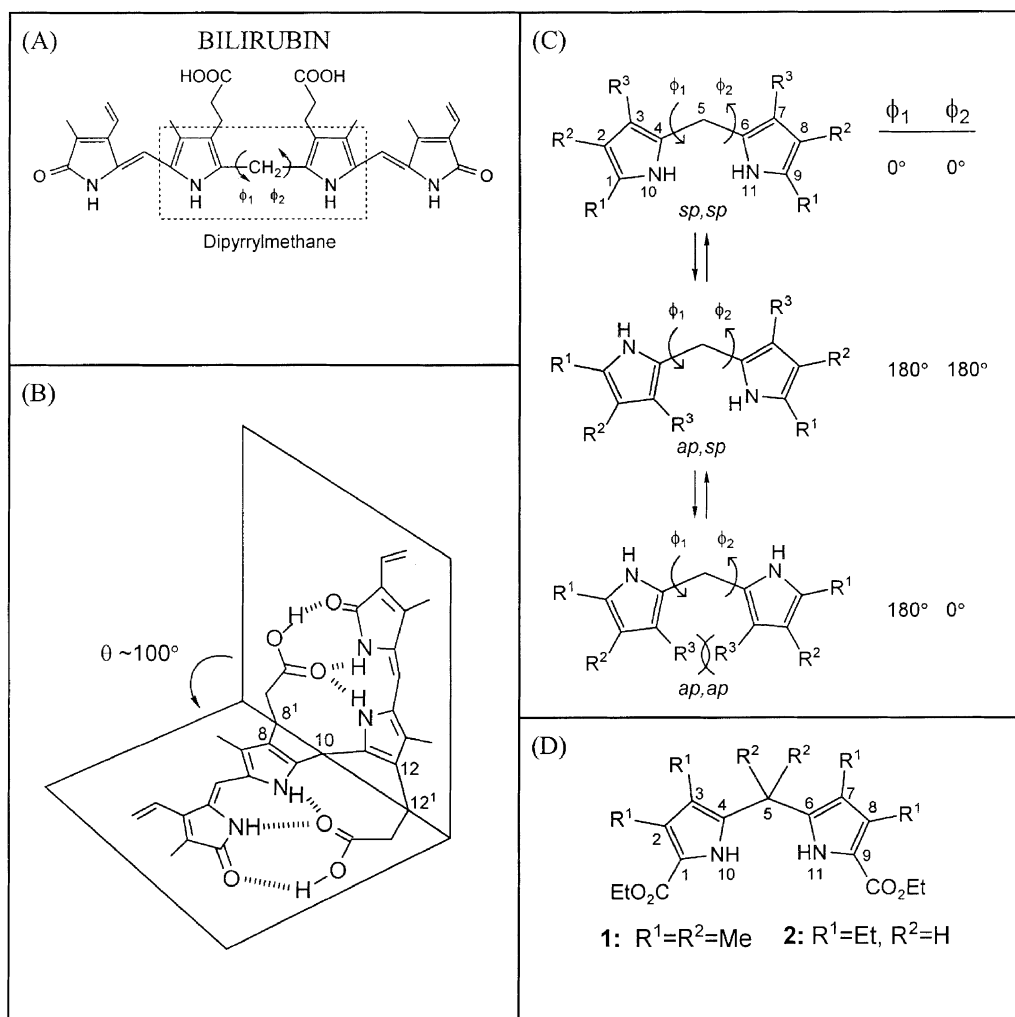


**Fig. 1.** Bilirubin has two dipyrinone chromophores; rotations about angles  $\phi_1$  and  $\phi_2$  interconvert various conformations, including (A), in a high energy linear conformational representation with angles of rotation about the C(9)-C(10) and C(10)-C(11) bonds,  $\phi_1$  and  $\phi_2$ ,  $\sim 180^\circ$ , and (B), the global energy minimum conformation shaped like a ridge-tile with  $\phi_1 = \phi_2 \sim 60^\circ$  and an interplanar angle of  $\sim 100^\circ$ . The ridge-tile seam in (B) lies approximately along the line connecting 8<sup>1</sup>, 10, and 12<sup>1</sup>; this conformation achieves considerable stabilization from intramolecular hydrogen bonds (hatched lines). (C) Periplanar dipyrrolylmethane conformations obtained by rotations about  $\phi_1$  and  $\phi_2$ . Conformations where  $30^\circ < \phi_1, \phi_2 < 150^\circ$  are typically slightly more stable than the periplanar one. (D) Target *gem*-dimethyl dipyrrolylmethane **1** and a simpler analog (**2**) with no *gem*-dimethyl moiety

The gable conformation (Fig. 2) has been computed to be energetically favored in the simple molecular propeller diphenylmethane [9]. However, the gable conformer is only by *ca.* 0.84 kJ/mol more stable than a  $C_2$ -propeller where  $\phi_1 \sim \phi_2 \sim 45^\circ$ , and so the conformational equilibrium can be expected to be easily perturbed. The presence of a *gem*-dimethyl group, for example, tilts the equilibrium relatively strongly toward a  $C_2$ -propeller ( $\phi_1 \sim \phi_2 \sim 50^\circ$ ) and away from the gable ( $C_{2v}$ ) conformation [9]. One

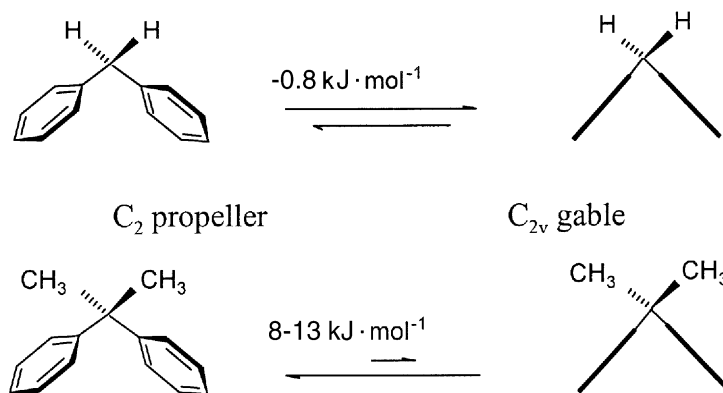


**Fig. 2.** (Upper) Diphenylmethane conformations with the  $\text{C}_{2v}$  gable geometry being slightly favored over the  $\text{C}_2$  propeller; (Lower) 2,2-Diphenylpropane conformations with the  $\text{C}_2$  propeller geometry more substantially favored

might anticipate a similar behavior in pyrrole analogs, especially for the parent dipyrromethane and its *gem*-dimethyl analog, but dipyrromethanes of greatest interest are those where the pyrrole rings have  $\beta$ -substituents and thus are structurally closest to the dipyrromethane unit in bilirubin (Fig. 1A). Among the periplanar conformations (Fig. 1C), the *sp,sp* conformer might be expected to be more stable than either *ap,sp* or *ap,ap*, with the latter being destabilized by a nonbonded steric interaction between the  $R^3$  groups. Earlier conformational analysis of the simple dipyrromethane ( $R^1 = R^2 = R^3 = \text{H}$ , Fig. 1C) [2, 10] revealed broad, connected regions of conformational stability on a conformational energy map obtained by independent rotations about  $\phi_1$  and  $\phi_2$ . Conformational energies differ by only *ca.* 0.84 kJ/mol, and minima were found near  $\phi_1, \phi_2 \sim 75^\circ, 55^\circ$  (*sc,sc*),  $\phi_1, \phi_2 \sim 235^\circ, 70^\circ$  (*ac,sc*),  $\phi_1, \phi_2 \sim 115^\circ, 95^\circ$  (*ac,ac*), *etc.* Ring substituents alter the picture somewhat. For example with pyrrole  $\beta$ -methyls, as in  $R^1 = R^2 = \text{H}$ ,  $R^3 = \text{Me}$  of Fig. 1C, a global minimum is found at  $\phi_1 \sim 105^\circ$ ,  $\phi_2 \sim 35^\circ$  lying in a broad valley of shallow isoenergy curves [11]. When  $R^1 = \text{CO}_2\text{Et}$ ,  $R^2 = R^3 = \text{Me}$ , the global minimum is computed [12] to be  $\phi_1 \sim -120^\circ$ ,  $\phi_2 \sim +40^\circ$ ; when  $R^1 = \text{CO}_2\text{Et}$ ,  $R^2 = R^3 = \text{Et}$ , it is computed to lie at  $\phi_1 \sim -95^\circ$ ,  $\phi_2 \sim 65^\circ$  [2,11]. Apparently, when  $R^3 = \text{alkyl}$ , the *-ac,+sp* conformation is energetically preferred. The energetic minima do not quite correspond to a gable conformation, although other propeller conformations lie energetically close by. Just how a *gem*-dimethyl group might affect the dipyrromethane conformation was unknown, and whether it might affect the conformational selection as it does in diphenylmethanes was unclear.

Consequently, we synthesized **1** (Fig. 1D), a *gem*-dimethyl analog of **2**, analyzed its conformation by molecular mechanics calculations, and obtained its crystal structure by X-ray analysis. To the best of our knowledge, the crystal structure is only the third of a simple dipyrromethane. The first was obtained over 25 years ago by *Bonnett et al.* [13] on **2**. More recently, a crystal structure was obtained on an N-N trimethylene-bridged dipyrromethane, whose conformation ( $\phi_1 \sim \phi_2 \sim 90^\circ$ ,  $\theta \sim 111^\circ$ ) is governed by that of its eight-membered ring [14].

## Results and Discussion

### Synthetic aspects

The synthesis of **1** proceeded smoothly from the known monopyrrole ethyl 3,4-dimethylpyrrole-2-carboxylate (**3**) [15a, 16] by modification of the method of *Hong* and *Smith* [17] who coupled the benzyl ester of **3** with acetone in 65–75% yield using boron trifluoride etherate as catalyst. We found that **3** could be coupled to give a >90% yield of **1** by *p*-toluenesulfonic acid catalyzed condensation with 2,2-dimethoxypropane. The use of acetone with catalysts such as boron trifluoride etherate or sulfuric acid was less satisfactory [18].

### Configuration and overall conformation

An examination of the crystal structure drawing of **1** clearly indicates that the molecule adopts an *ac,ac* conformation where the pyrrole NHs are oriented *syn* to the *gem*-dimethyl group. The molecule is not planar; the pyrrole rings are rotated in a propeller fashion by  $\sim 35$ – $45^\circ$  out of planarity (Fig. 3). This conformation differs significantly from that found for **2**, which lacks a *gem*-dimethyl group. Dipyrrolylmethane **2** adopts a gable-like conformation while being arranged in the crystal lattice as intermolecularly hydrogen-bonded centrosymmetrically related dimers [2, 13]. One ester group of **2** is *syn*-periplanar to the adjacent pyrrole-NH, as is required for the intermolecular hydrogen bonding in the crystal. The other is *anti*-periplanar, which is the energetically favored conformation in pyrrole esters with  $\beta$ -alkyls [12] in the absence of hydrogen bonding. Intermolecular hydrogen bonding in the crystal appears to be an important factor in favoring a *syn*-periplanar arrangement in ethyl 3,4-diethyl-pyrrole-2-carboxylate [19].

The *gem*-dimethyl of **1** affects the interplanar angle. Although the two planes containing the two pyrroles in **1** and in **2** intersect at similar interplanar angles,  $\theta \sim 104^\circ$  in **1** and  $\sim 72^\circ$  in **2**, the dihedral angle of **1** is only slightly larger than that found in bilirubin [20a,b] ( $\theta \sim 100^\circ$ ) and is comparable to that reported for mesobilirubin [20c] ( $\theta \sim 104^\circ$ ). However, the orientation of the pyrrole rings differs substantially. In bilirubin and mesobilirubin the NHs are oriented *anti* relative to

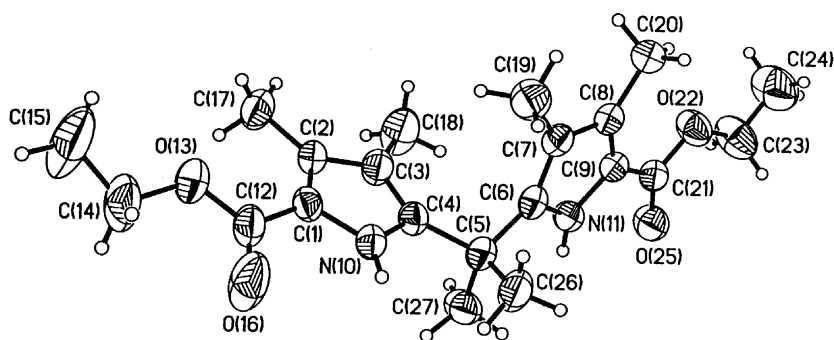
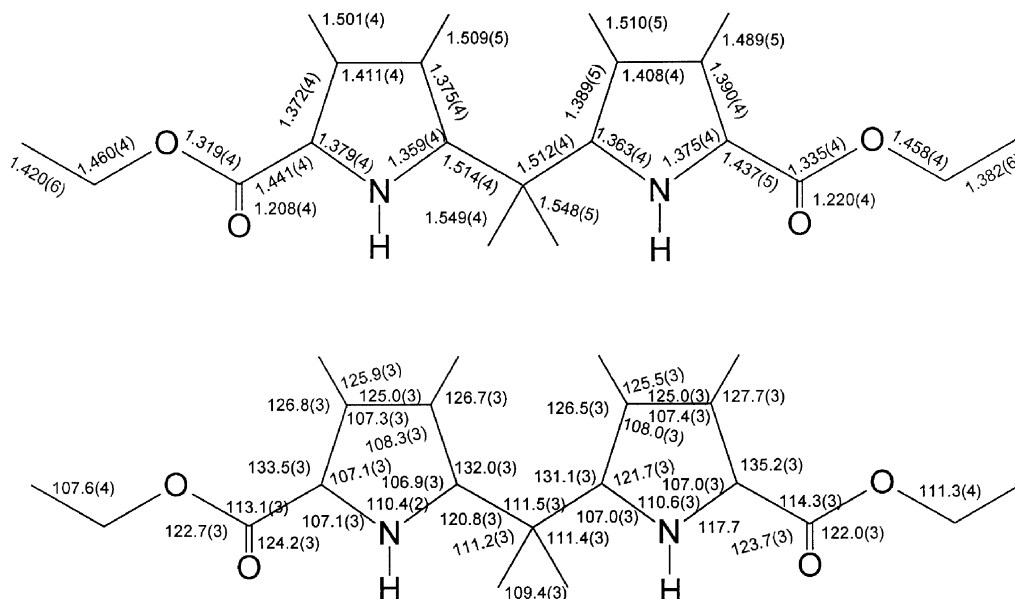
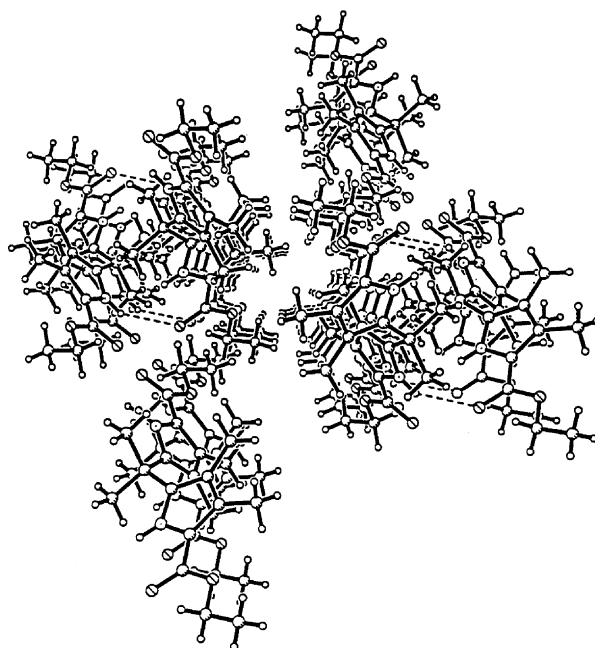


Fig. 3. Structural drawing of **1** (crystal structure) with hydrogens located; thermal ellipsoids have been drawn to 50% probability





**Fig. 5.** Molecular packing of molecules of **1** in a projection as viewed along the *b* axis. For ease of viewing, long intermolecular hydrogen bonds are shown by dashed lines. However, it is not clear if the interaction can be rigidly defined as a hydrogen bond since the N to O nonbonded distance is 3.10 Å, or less than the sum (2.90 Å) of the *van der Waals* radii of N and O

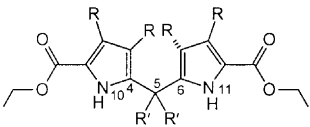
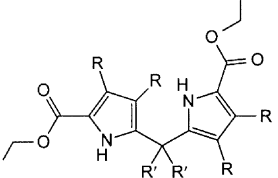
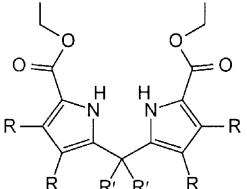
### *Crystal packing*

The stacking pattern in **1** (Fig. 5) clearly differs from that found in its analog **2** without *gem*-dimethyls [13] and in bilirubin [6,20]. In **1** propellers are stacked with a pyrrole ring of one molecule squarely atop and parallel to a pyrrole ring of a second molecule, some 11 Å distant. There is little evidence for hydrogen bonding in crystals of **1**. The closest intermolecular approach of one of the NHs to an ester C=O is ~3.1 Å for the N to O nonbonded distance of the only possible intermolecular N–H···O=C hydrogen bond. Since the N to O nonbonded distance is less than the sum of the *van der Waals* radii of nitrogen and oxygen (2.90 Å), it is not clear that this interaction can be rigidly defined as a hydrogen bond. Nonetheless, for ease of viewing of the packing diagram, such long intermolecular hydrogen bonds are shown in Fig. 5 as dashed lines. From the hydrogen bonding perspective, the structure of **1** thus differs in yet another important way from that of **2**, which packs in its crystal as hydrogen-bonded, centrosymmetrically related dimers.

### *Conformation from molecular mechanics calculations*

Insight into the preferred conformations of dipyrromethanes and the *gem*-dimethyl analog **1** and the influence of the *gem*-dimethyl group on conformation may be obtained from molecular mechanics computations as well as by crystallography. Torsion angles (C–C) about the carbon-carbon bonds linking the two rings are

**Table 1.** Comparison of conformation determining torsion angles ( $^{\circ}$ ) from X-ray crystallography and molecular mechanics (MM)<sup>a</sup> calculations for **1** and **2** and bilirubin

	Method of Analysis	Torsion angle ( $^{\circ}$ )		Heat of formation (kJ/mol) <sup>a</sup>
		$\phi_1$ (6-5-4-1)	$\phi_2$ (4-5-6-11)	
<b>1</b> : $R = R' = \text{Me}$				
<b>2</b> : $R = \text{Et}$ , $R' = \text{H}$				
	<b>1</b> X-ray	-147	-135	-
	<b>2</b> X-ray <sup>b</sup>	-94	+67	-
	<b>1</b> MM	-133	-133	-523
	<b>2</b> MM	-121	-117	-558
	<b>1</b> MM	-122	+21	-517
	<b>2</b> MM	-94	+37	-560
	<b>1</b> MM	-33	-33	-501
	<b>2</b> MM	-80	-55	-552

<sup>a</sup> Using PCModel vers.7.0, ref. [12]:  $\Delta H_f$  values are higher when the ester carbonyl conformation is *sp* or *sc* to the pyrrole nitrogen, <sup>b</sup> Data taken from X-ray diffraction coordinates given in Ref. [12]

mainly responsible for determining the conformation and helicity. These torsion angles and the helical pitch can be extracted from atomic coordinates of the minimum energy conformation determined by molecular orbital and molecular dynamics calculations [2, 10, 11] and by crystallography [13]. Comparison of the torsion angles obtained from both techniques for **1** and **2** are shown in Table 1, and a full list of torsion angles of **1** may be found in Table 2.

As shown previously, the conformational energy map of dipyrromethanes consists of broad valleys with only small energy differences among various propeller conformations [2, 10, 11]. Interestingly, molecular mechanics calculations, which do not take into account crystal packing forces, predict a global energy minimum *ac,ac* conformation for **1** with torsion angles rather similar to those found in the crystal. The global minimum lies some 5.8–21 kJ/mol lower in energy than either an *-ac,+sp* or *sc,sc* conformation. In contrast, the *-ac,+sp* conformation favored in crystals of **2** is predicted to lie at the global energy minimum, some 1.7 kJ/mol below the *-ac,-ac* and  $\sim 7.5$  kJ/mol below the *sp,sp* conformation. These differences are small in **2** but much larger in **1**, emphasizing the importance of the *gem*-dimethyl group in conformational selection. The calculations also reproduce the experimental torsion angles reasonably well, predicting slightly smaller torsion angles ( $\phi_1$  and  $\phi_2$ ) in **1** and **2**. The conformational bias, where the NH and *gem*-dimethyls of **1** are *syn*

**Table 2.** Torsion angles (°) for **1**

N(10)-C(1)-C(2)-C(3)	-0.5(4)	C(19)-C(7)-C(8)-C(9)	-177.4(3)
C(12)-C(1)-C(2)-C(3)	-172.7(4)	C(6)-C(7)-C(8)-C(20)	-179.7(3)
N(10)-C(1)-C(2)-C(17)	-177.6(3)	C(19)-C(7)-C(8)-C(20)	2.5(5)
C(12)-C(1)-C(2)-C(17)	5.4(6)	C(7)-C(8)-C(9)-N(11)	-0.3(3)
C(1)-C(2)-C(3)-C(4)	0.0(4)	C(20)-C(8)-C(9)-N(11)	179.7(3)
C(17)-C(2)-C(3)-C(4)	-178.2(4)	C(7)-C(8)-C(9)-C(21)	-177.2(3)
C(1)-C(2)-C(3)-C(18)	177.7(4)	C(20)-C(8)-C(9)-C(21)	2.8(6)
C(17)-C(2)-C(3)-C(18)	-0.5(6)	C(3)-C(4)-N(10)-C(1)	-0.9(4)
C(2)-C(3)-C(4)-N(10)	0.6(4)	C(5)-C(4)-N(10)-C(1)	-176.0(3)
C(18)-C(3)-C(4)-N(10)	-177.1(4)	C(2)-C(1)-N(10)-C(4)	0.9(3)
C(2)-C(3)-C(4)-C(5)	174.9(3)	C(12)-C(1)-N(10)-C(4)	174.5(3)
C(18)-C(3)-C(4)-C(5)	-2.8(6)	C(7)-C(6)-N(11)-C(9)	0.1(3)
N(10)-C(4)-C(5)-C(6)	-146.5(3)	C(5)-C(6)-N(11)-C(9)	-174.8(3)
C(3)-C(4)-C(5)-C(6)	39.9(5)	C(8)-C(9)-N(11)-C(6)	0.2(3)
N(10)-C(4)-C(5)-C(27)	92.0(4)	C(21)-C(9)-N(11)-C(6)	177.7(3)
C(3)-C(4)-C(5)-C(27)	-81.6(4)	C(2)-C(1)-C(12)-O(16)	165.1(4)
N(10)-C(4)-C(5)-C(26)	-26.8(4)	N(10)-C(1)-C(12)-O(16)	-6.4(6)
C(3)-C(4)-C(5)-C(26)	159.6(4)	C(2)-C(1)-C(12)-O(13)	-13.0(6)
C(4)-C(5)-C(6)-N(11)	-134.8(3)	N(10)-C(1)-C(12)-O(13)	175.5(3)
C(27)-C(5)-C(6)-N(11)	-16.4(4)	O(16)-C(12)-O(13)-C(14)	-4.3(6)
C(26)-C(5)-C(6)-N(11)	103.3(4)	C(1)-C(12)-O(13)-C(14)	173.8(3)
C(4)-C(5)-C(6)-C(7)	51.8(5)	C(12)-O(13)-C(14)-C(15)	172.4(5)
C(27)-C(5)-C(6)-C(7)	170.1(3)	N(11)-C(9)-C(21)-O(25)	-1.7(5)
C(26)-C(5)-C(6)-C(7)	-70.2(4)	C(8)-C(9)-C(21)-O(25)	174.9(3)
N(11)-C(6)-C(7)-C(8)	-0.3(3)	N(11)-C(9)-C(21)-O(22)	178.9(3)
C(5)-C(6)-C(7)-C(8)	173.9(3)	C(8)-C(9)-C(21)-O(22)	-4.4(5)
N(11)-C(6)-C(7)-C(19)	177.5(3)	O(25)-C(21)-O(22)-C(23)	-4.2(5)
C(5)-C(6)-C(7)-C(19)	-8.3(6)	C(9)-C(21)-O(22)-C(23)	175.2(3)
C(6)-C(7)-C(8)-C(9)	0.4(3)	C(21)-O(22)-C(23)-C(24)	-178.8(4)

suggest an explanation for the unusual increased amphiphilic properties of a bilirubin analog with 10,10-dimethyls [16].

## Experimental

All NMR spectra were obtained on a GE QE-300 300 MHz spectrometer, or on a Varian Unity Plus 500 MHz spectrometer. Chemical shifts are reported in  $\delta$  (ppm) referenced to the residual  $\text{CHCl}_3$   $^1\text{H}$  signal at 7.26 ppm and the corresponding  $^{13}\text{C}$  signal at 77.0 ppm. Mass spectra were obtained on an H-P 5890 GC-mass spectrometer. Melting points were taken on a Mel-temp capillary apparatus and the uncorrected. The combustion analysis of **1**, determined by Desert Analytics, Tucson, AZ, is in satisfactory agreement with the calculated values. Analytical thin layer chromatography was performed on J.T. Baker silica gel IB-F plates (125  $\mu$  layers). Flash vacuum column chromatography was carried out using Woelm silica gel F, thin layer chromatography grade. Spectroscopic data were obtained in spectral grade solvents (Aldrich or Fisher). 2,2-Dimethoxypropane and *p*-toluenesulfonic acid were purchased from Aldrich; dichloromethane and hexane were Fisher.



**Table 3.** Crystallographic data for *gem*-dimethyl dipyrromethane

Formula weight	374.47
Crystallized from	CH <sub>2</sub> /Cl <sub>2</sub> / <i>n</i> -hexane
Temperature (K)	298(2) K
Crystal size (mm)	0.34×0.48×0.46
Formula	C <sub>21</sub> H <sub>30</sub> N <sub>2</sub> O <sub>4</sub>
Space group	<i>C2/c</i>
<i>Z</i>	8
Cell dimension	<i>a</i> = 25.908(3) Å <i>b</i> = 11.0770(10) Å <i>c</i> = 16.827(3) Å $\alpha = 90^\circ$ $\beta = 118.330(10)^\circ$ $\gamma = 90^\circ$ <i>V</i> = 4250.7(10) Å <sup>3</sup>
No. $\theta$ range of Refs. used for cell refinement	27 / $1.78^\circ < \theta < 12.49^\circ$
Calc. density <i>d<sub>x</sub></i> (g/cm <sup>3</sup> )	1.170
Data collection range	$35^\circ < 2\theta < 50^\circ$
Scan type/scan range	<i>w</i> /1.1°
No. of total data recorded	4458
No. of unique data	3735
Weighting scheme <sup>a</sup>	<i>a</i> = 0.112, <i>b</i> = 0
No. of obs/No. of parameters	3735/253
<i>R</i> <sub>1</sub> <sup>b</sup> , <i>wR</i> <sub>2</sub> <sup>c</sup> ( <i>I</i> > 2σ( <i>I</i> ))	<i>R</i> <sub>1</sub> = 0.0709, <i>wR</i> <sub>2</sub> = 0.1985
e.s.d. of C-C bondlength	0.004
Highest peak in final Δ <i>F</i> -map (e Å <sup>-3</sup> )	0.414
Anisotropic non-H atoms	all
Isotropic non-H atoms	none
μ(MoKα) (mm <sup>-1</sup> )	0.081
Radiation (λ, Å)	0.71073
Transmission factors	0.7595–0.7211

<sup>a</sup> $w^{-1} = (\sigma^2(F_o^2) + (aP)^2 + bP)$  where  $P = (F_o^2 + 2F_c^2)/3$ ; goodness of fit (GOOF):  $(\sum(w(F_o^2 - F_c^2)^2)/(M - N))^{0.5}$  where *M* is the number of reflections and *N* is the number of parameters refined; <sup>b</sup> $R_1 = \sum||F_o| - |F_c||/\sum|F_o|$ ; <sup>c</sup> $wR_2 = (\sum[w(F_o^2 - F_c^2)^2]/\sigma(w(F_o^2)^2))^{0.5}$

*Diethyl-2,3,5,5,7,8-hexamethyl-5,10-dihydrodipyrin-1,9-dicarboxylate (1, C<sub>21</sub>H<sub>30</sub>N<sub>2</sub>O<sub>4</sub>)*

2-Carboethoxy-3,4-dimethyl-1*H*-pyrrole, prepared as described previously [15, 16] (1.67 g, 10.0 mmol), was dissolved in 50 cm<sup>3</sup> of CH<sub>2</sub>Cl<sub>2</sub> at room temperature with magnetic stirring. 2,2-Dimethoxypropane (3.2 cm<sup>3</sup>, ~26 mmol) was added to the solution along with ~150 mg (0.87 mmol) of *p*-toluenesulfonic acid catalyst. The reaction mixture was stirred at room temperature for 24 h, the reaction progress being monitored by TLC. The reaction was quenched with 100 cm<sup>3</sup> of H<sub>2</sub>O; then, 0.5 g of NaHCO<sub>3</sub> were added, and the mixture was shaken. The organic layer was separated, the aqueous layer was extracted three times with 10 cm<sup>3</sup> of CH<sub>2</sub>Cl<sub>2</sub> each, and the combined organic layers were dried over anhyd. MgSO<sub>4</sub>. After evaporation of the solvent, the dark residue was flash vacuum chromatographed using CH<sub>2</sub>Cl<sub>2</sub>, then 1% (by vol.) methanol in CH<sub>2</sub>Cl<sub>2</sub> as eluent. After evaporation of the solvent, the remaining solid was crystallized from CH<sub>2</sub>Cl<sub>2</sub>-hexane to yield colorless granular crystals.

Yield: 1.7 g (90%); mp.: 122–124°C; IR (KBr):  $\nu = 3450, 3355, 2980, 2930, 1685, 1665, 1490, 1430, 1365, 1270, 1190, 1135, 1090, 1025, 945, 775 \text{ cm}^{-1}$ ;  $^1\text{H NMR}$  ( $\text{CDCl}_3$ ,  $\delta$ , 300 MHz): 1.37 (t,  $J = 7.2$ , 6H), 1.54 (s, 6H), 1.66 (s, 6H), 2.21 (s, 6H), 4.31 (q,  $J = 7.2$ , 4H), 8.59 (br s, 2H) ppm;  $^{13}\text{C NMR}$  ( $\text{CDCl}_3$ ,  $\delta$ , 125 MHz): 9.20 (q), 10.45 (q), 14.64 (q), 26.78 (q), 35.84 (s), 59.80 (t), 116.0 (s), 116.9 (s), 128.3 (s), 137.1 (s), 161.9 (s) ppm; MS:  $m/z = 374$  ( $\text{M}^+$ ), 359, 313, 267, 208, 207, 162.

#### *X-Ray structure analysis*

Crystals of **1** were grown from a solution of  $\text{CH}_2\text{Cl}_2$ -hexane by slow evaporation. Suitable crystals were coated with epoxy cement, mounted on a glass fiber, and placed on a Siemens P4 diffractometer. Unit cell parameters were determined by least squares analysis of 27 reflections with  $1.78^\circ < \theta < 12.49^\circ$  using graphite monochromatized  $\text{MoK}_\alpha$  radiation ( $0.71073 \text{ \AA}$ ). 4458 reflections were collected between  $3.5 < 2\theta < 50^\circ$  yielding 3735 unique reflections ( $R_{\text{int}} = 0.0239$ ). The data were corrected for *Lorentz* and polarization effects. Crystal data are given in Table 3. Scattering factors and corrections for anomalous dispersion were taken from a standard source [22].

Calculations were performed using Siemens SHELXTL PLUS, version 5.03, refining on  $F^2$ . The structure was solved by direct methods in the space group,  $C2/c$ . The unit cell contains an ordered array of the molecule with no unusual contacts.

**Table 4.** Atomic coordinates ( $\times 10^4$ ) and equivalent isotropic displacement parameters ( $\text{\AA}^2 \times 10^3$ ) for **1**;  $U(\text{eq})$  is defined as one third of the trace of the orthogonalized  $U^{ij}$  tensor

	<i>x</i>	<i>y</i>	<i>z</i>	<i>U</i> (eq)
C(1)	1631(1)	310(3)	3105(2)	52(1)
C(2)	1247(1)	305(3)	2197(2)	58(1)
C(3)	1318(2)	1410(3)	1842(2)	62(1)
C(4)	1742(1)	2070(3)	2537(2)	52(1)
C(5)	2031(1)	3264(3)	2554(2)	61(1)
C(6)	1594(2)	4163(3)	1909(2)	47(1)
C(7)	1056(2)	4548(3)	1807(2)	58(1)
C(8)	855(1)	5491(3)	1170(2)	58(1)
C(9)	1273(1)	5666(3)	885(2)	54(1)
C(10)	1932(1)	1388(2)	3296(2)	53(1)
C(11)	1716(1)	4850(2)	1346(2)	57(1)
C(12)	1805(2)	−587(3)	3806(3)	68(1)
C(13)	1458(1)	−1540(2)	3559(2)	82(1)
C(14)	1636(2)	−2549(4)	4193(3)	107(2)
C(15)	1170(3)	−3400(5)	3856(4)	172(3)
C(16)	2232(2)	−503(3)	4539(2)	133(2)
C(17)	839(2)	−698(3)	1666(3)	90(1)
C(18)	995(2)	1764(4)	859(2)	101(2)
C(19)	728(2)	4024(4)	2266(3)	84(1)
C(20)	293(2)	6157(3)	872(3)	73(1)
C(21)	1343(2)	6494(3)	286(2)	57(1)
C(22)	892(1)	7245(2)	−149(2)	76(1)
C(23)	965(2)	8164(4)	−707(3)	100(2)
C(24)	478(2)	8904(5)	−1109(4)	130(2)
C(25)	1778(1)	6529(2)	181(2)	76(1)
C(26)	2311(2)	3836(3)	3508(2)	87(1)
C(27)	2517(2)	2979(3)	2295(3)	87(1)

All non-hydrogen atoms (Table 4) were refined with anisotropic thermal parameters. The data were corrected for absorption using an empirical model derived from  $\psi$  scans. Hydrogen atom positions were calculated using a riding model with a C-H distance fixed at 0.96 Å and a thermal parameter 1.2 times that of the host carbon atom. The largest peak in the final difference map corresponded to  $-0.223 \text{ e}/\text{Å}^3$  and was located 1.27 Å from C24. Tables of bond lengths and angles, anisotropic displacement parameters, hydrogen coordinates, and isotropic displacement parameters have been deposited at the Cambridge Structural Data file (CDC No. 138503).

## Acknowledgements

We thank the U.S. National Institutes of Health (HD-17779) for generous support of this work. Special thanks are accorded to Professor V. J. Catalano for his assistance with the X-ray crystallographic measurements and to Mr. M.T. Huggins and Dr. S. E. Boiadjev for advice on the syntheses. Derek Lightner was a participant in the NSF REU program in summer 1999.

## References

- [1] Berk PD, Noyer C (1994) Seminar in Liver Disease **14**: 321
- [2] Falk H (1989) The Chemistry of Linear Oligopyrroles and Bile Pigments. Springer, Wien
- [3] McDonagh AF (1979) Bile Pigments: Bilatrienes and 5,15-Biladienes. In: *The Porphyrins*, Dolphin D (ed) Academic Press, New York, Vol. 6, pp 293–491
- [4] Person RV, Peterson BR, Lightner DA (1994) J Am Chem Soc **116**: 42
- [5] Boiadjev SE, Pfeiffer WP, Lightner DA (1997) Tetrahedron **53**: 14547
- [6] For a review of crystal structures of linear polypyrrolic compounds, see Sheldrick WS (1983) Israel J Chem **23**: 155
- [7] (a) Kaplan D, Navon G (1983) Israel J Chem **23**: 177; (b) Kaplan D, Navon G (1983) Org Magn Res **17**: 79; (c) Kaplan D, Navon G (1982) Biochem J **201**: 605; (d) Navon G, Frank S, Kaplan D (1984) J Chem Soc Perkin Trans 2, 1145
- [8] Kuhn LP, Kleinspehn GG (1963) J Org Chem **28**: 721
- [9] Barnes JC, Paton JD, Damewood JR Jr, Mislow K (1981) J Org Chem **46**: 4975
- [10] Falk H, Müller N (1983) Tetrahedron **39**: 1875
- [11] Favini G, Pitea D, Manitto P (1979) Nouv J Chem **3**: 299
- [12] PCModel vers. 7.0 using the MMX forcefield, Serena Software, Bloomington, IN, USA
- [13] Bonnett R, Hursthouse MB, Neidle S (1972) J Chem Soc Perkin Trans 2: 1335
- [14] Timmermann R, Mattes R, Frank B (1987) Angew Chem **99**: 74
- [15] Kleinspehn GG (1955) J Am Chem Soc **77**: 1546
- [16] (a) Xie M, Lightner DA (1993) Tetrahedron **49**: 2185; (b) Xie M, Holmes DL, Lightner DA (1993) Tetrahedron **49**: 9235
- [17] Xie H, Smith KM (1992) Tetrahedron **33**: 1197; and Smith KM (private communication)
- [18] Xie M (1993) Total Synthesis and Structural Analysis of C(10) *gem*-Dimethyl Analogs of Mesobilirubin-XIII $\alpha$ , PhD Dissertation, University of Nevada, Reno
- [19] Bonnett R, Hursthouse MB, Neidle S (1972) J Chem Soc Perkin Trans 2, 902.
- [20] (a) Bonnett R, Davies JE, Hursthouse MB, Sheldrick GM (1978) Proc R Soc London, Ser B **202**: 249; (b) LeBas G, Allegret A, Mauguen Y, DeRango C, Bailly M (1980) Acta Cryst Sect B, **B36**: 3007; (c) Becker W, Sheldrick WS (1978) Acta Cryst Sect B, **B34**: 1298
- [21] Gatehouse BM, Craven BM (1971) Acta Cryst **B27**: 1337
- [22] Ibers JA, Hamilton WC (1974) International Tables for X-ray Crystallography, vol 4. Kynoch Press, Birmingham